both methods depending on the structure of the target derivatives. We summarize our synthesis of 4′-*C*-methyl, fluoromethyl and ethynyl nucleosides using the condensation method (Figure 8). We started our chemistry with the synthesis of 4′-*C*-methyl nucleosides (Ohrui *et al.*, 1991). These 4′-SNs [**27, 45, 61–70**] were prepared by the condensation method, which utilized a key intermediate, 4-*C*-methyl-D-ribofuranose derivative [**59**] (Waga *et al.*, 1993). During the preparation of a series of 2′-deoxynucleoside [**27, 61, 62**], 2′,3′-unsaturated nucleoside [**45, 66, 67**], 2′,3′-dideoxynucleoside [**68–70**] and ara-*C* analogues [**64**] by the above method, we found that 4′-*C*-methyl-2′-deoxycytidine (4′-MdC) [**27**] showed inhibitory activity against HIV in MT-4 cells (Waga *et al.*, 1996).

Although 4′-MdC [**27**] was 100-fold more potent than the thymidine derivative 4′-MT [**61**], it was the most cytotoxic compound among the 4′-*C*-methyl nucleosides tested. Interestingly, the 4′-MdC [**27**] was also tested for its ability to inhibit the growth of P388 mouse leukaemia cells, and it proved to be markedly effective (IC_{50}=1.7 μM). The mechanism of action of [**27**] was also studied (Yamaguchi *et al.*, 1997).

Since the Yamasa Corporation developed BVaraU as an anti-HSV-1 drug, we prepared 4′-*C*-methyl-BVaraU [**65**] and 4′-*C*-methyl-BVDU [**63**] as antiviral agents. Compound [**63**] exhibited particularly potent anti-HSV-1 and anti-varicella-zoster virus (VZV) activity (Kitano *et al.*, 1999). Additionally, 4′-*C*-fluoromethyl nucleosides such as 2-deoxy-D-erythro- and *arabino*-pentofuranosyl cytosine [**73,74**] were previously synthesized by us using an analogous method (Kitano *et al.*, 1997). Interestingly, 4′-*C*-fluoromethyl-2′-deoxycytidine (4′-FMdC) [**73**] exhibited not only potent anti-HIV activity but also anti-neoplastic activity.

As mentioned above, 4′-ethynyl-pyrimidine-nucleosides showed anti-HIV activity. However, there were only a few reports on the preparation of 4′-ENs. Moreover, those papers did not mention any synthetic method of 4′-ENs, especially in the case of purine nucleosides. Thus, we started the chemistry for modifying the 4′-*C*-position of purine nucleosides with an ethynyl group. 4′-ENs could be prepared from the corresponding nucleosides, but we usually used 4-*C*-hydroxymethyl-3,5-di-*O*-benzyl-1,2-*O*-isopropylidene-α-D-*ribo*-furanose [**75**] as a versatile starting material for the synthesis of D-arabino and 2′-deoxy-D-ribo analogues of 4′-ENs [**77–80**]. The outline of our study for the synthesis of 4′-ENs is shown in Figure 8 (Kohgo *et al.*, 1999), and the anti-HIV activity is summarized in Figure 9 and Table 1 (Maag *et al.*, 1992; O-Yang *et al.*, 1999; Nomura *et al.*, 1999; Sugimoto *et al.*, 1999; Ohrui *et al.*, 2000; Ohri *et al.*, 2001).

Since 4′-*C*-substituted nucleosides showed anti-HIV activity (Table 1), we decided to explore the novel NRTIs

Figure 9. Structures of 4′-*C*-substituted nucleosides*

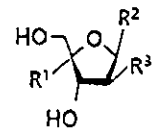

*See Table 1 for anti-HIV activity of R^1, R^2 and R^3.

that are active against drug-resistant HIV-1 variants and that prevent or delay the emergence of resistant HIV-1.

Summary of SARs of 4′-SNs against HIV-1

As described in other research groups' investigations, the syntheses and anti-HIV activity of 4′-*C*-methyl-thymidine (4′-MT) [**61**], 4′-*C*-ethynyl-2′-deoxycytidine (4′-EdC) [**22**], 4′-*C*-ethyl-2′-deoxycytidine (4′-EtdC) [**24**], 4′-*C*-ethynyl-thymidine (4′-ET) [**28**] and some other 4′-SdNs were reported while we were working on our project. Therefore, SAR of various 4′-*C*-substituted nucleosides against HIV-1 are summarized together with our data:

1) The estimated relative order of anti-HIV-1 potency is as follows: $CN \geq N_3 \geq C{\equiv}CH > CH{\equiv}CH_2 > Me > Et > C{\equiv}C\text{-}Me$. This is based on published data. Interestingly, the order is the reverse of the $-\Delta G^0$ values between equatorial and axial substituents on a cyclohexane ring: $CN < F < C{\equiv}CH < CH{=}CH_2 < Me \leq Et < t\text{-}Bu$. Thus, these results indicate that the structure of 4′-SNs with a less sterically demanding substituent at the 4′-position is closer to the structure of dNs and has greater anti-HIV activity.

2) Purine analogues are generally less toxic than pyrimidine analogues; the former generally have greater selectivity indices (SI).

3) Ribo-derivatives are inactive, and arabino-derivatives are inactive or weakly active compared with 2′-deoxyribo counterparts.

4) 2′,3′-Dideoxyribo derivatives, including d4 type derivatives, with some exceptions do not show anti-HIV activity.

Design for creating novel NRTIs

One of our collaborators (Ohrui, 2001) speculated that the expected chemical and biological mechanisms of novel NRTIs were as follows:

1) The expected properties come from the presence of a 3′α-OH group.

Table 1. Anti-HIV activity of various 4'-*C*-substituted pyrimidine and purine nucleosides

Compound			Anti-HIV activity		
R^1	R^2	R^3	EC_{50} (μM)	CC_{50} (μM)	SI
CN	thymine	H	0.002	1	500
N_3	thymine	H	0.01	8	800
ethynyl	thymine	H	0.61	>380	>623
ethynyl	thymine	OH	>350	>350	–
ethynyl	5-ethyluracil	H	>360	>360	–
ethynyl	uracil	H	>100	>100	–
ethynyl	5-fluorouracil	H	>10	3.4	–
ethynyl	5-chlorouracil	H	6.0	81.7	13.6
ethynyl	5-bromouracil	H	2.3	>100	>43.5
ethynyl	5-iodouracil	H	0.34	>260	>765
CH_2N_3	thymine	H	2.1	333	159
Me	thymine	H	7.2	104	14.4
Et	thymine	H	16.1	>100	6.21
OMe	thymine	H	8.49	200	23.6
vinyl	thymine	H	6.1	>100	>16.4
hydroxyethyl	thymine	H	>4.7	4.7	–
propynyl	thymine	H	>100	>100	–
CN	cytosine	H	0.0012	0.17	142
N_3	cytosine	H	0.01	8	800
ethynyl	cytosine	H	0.0048	0.92	192
ethynyl	cytosine	OH	0.0048	1.74	363
ethynyl	5-methylcytosine	H	0.011	0.70	63
ethynyl	5-fluorocytosine	H	0.030	>100	>3333
ethynyl	5-chlorocytosine	H	>100	>100	–
ethynyl	5-bromocytosine	H	>100	>100	–
ethynyl	5-iodocytosine	H	>100	>100	–
Me	cytosine	H	0.015	1.0	66.7
CH_2F	cytosine	H	0.0068	0.12	18
Et	cytosine	H	0.013	0.77	59
vinyl	cytosine	H	0.0086	0.18	21
chlorovinyl	cytosine	H	2.1	4.6	2.2
N_3	adenine	H	0.13	50	385
ethynyl	adenine	H	0.098	16	1630
ethynyl	adenine	OH	0.78	248	318
ethynyl	2,6-diaminopurine	H	0.00034	0.9	2600
ethynyl	hypoxanthine	H	0.13	137	1053
ethynyl	guanine	H	0.0015	1.4	933
ethynyl	purine	H	135	>400	>3
methyl	adenine	H	2.6	2.6	–
	zidovudine (AZT)		0.0032	29.4	9190
	lamivudine (3TC)		0.10	>100	933

Figure 10. Speculations on how to overcome NRTIs' problems

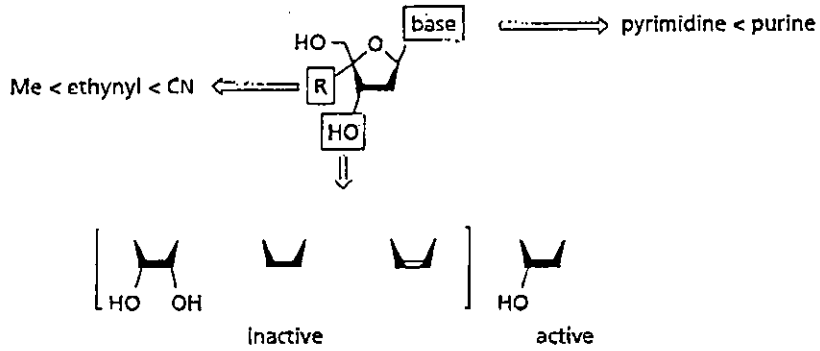

Figure 11. Synthetic problems of 4'-C-substituted nucleosides by condensation method

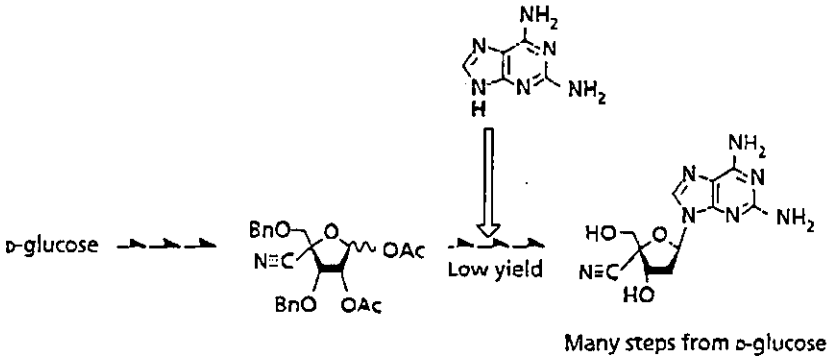

2) The presence of 3'α-OH in 4'-SdNs makes it acceptable by RTs and, therefore, 4'-SdNs are incorporated into the proviral DNA chains. The electron-withdrawing 3'α-OH group makes 4'-SdNs acid-stable even with purines. Thus, various purine derivatives can be made.

3) The expected properties come from the presence of 4'-substituents.

4) The 4'-substituents cause severe steric hindrance to the neighbouring *cis* 3'α-OH group due to restricted rotation around the C3'-C4' single bond. Thus, the reactivity of 3'α-OH sharply decreases. Therefore, it was expected that enzymatic chain elongation of DNA would not proceed by using the very unreactive 3'α-OH. Consequently, 4'-SdNs could be chain terminators for proviral DNA biosynthesis. The steric repulsion between 3'α-OH and 4'-substituents changes the conformation of the furanose ring of 4'-SdNs, preferably to 3'-endo conformation (N-Type); this results in 4'-SdNs being less susceptible to enzymatic degradation. Therefore, 4'-SdNs would be more stable than 2'-deoxynucleosides (dN) and 2',3'-dideoxynucleosides (ddN) against catabolism. The lipophilic substituent at the 4'-position imparts more lipophilicity to 4'-SdNs thus enabling them to penetrate the cell membrane efficiently. Possibly, this may enhance oral bioavailability and penetration through the

blood–brain barrier, although formal testing is needed to ascertain these issues. The emergence of highly resistant HIV-1 variants may not readily arise since the active anti-HIV 4′-SdNs with a smaller substituent at the 4′-position have structures more similar to dN.

If this speculation is true, we can design and discover novel NRTIs which are able to prevent, or delay, emergence of drug-resistant virus.

Design and synthesis of 4′-CNdNs from natural 2′-deoxynucleosides

From previous studies on SAR of 4′-*C*-substituted nucleosides, it was expected that a smaller substituent at the *C*-4′ position would give more acceptable biological activity. This is based on the parameter $-\Delta C^{\circ}$ values between equatorial and axial substituents on the cyclohexane rings. Thus, purine 2′-deoxynucleoside derivatives bearing a cyano group, which might be smaller than an ethynyl one (at the *C*-4′-position), will have more potent antiviral activity. During our synthesis of 4′-*C*-substituted nucleosides, we have been utilizing a glycosidation reaction of 4-*C*-substituted sugar derivatives with nucleobases. However, this synthetic route incurs some problems (Figure 11).

Synthetic problems in the condensation method are summarized as follows:

1) Preparation of 4′-*C*-substituted sugars and their derivation to the desired nucleosides require multi-step reactions and their total yields are low.

2) 4′-*C*-Substituted sugars have low reactivity in glycosidation reaction, especially when their substituent is an electron-withdrawing group like a cyano group.

These problems prompted us to develop a preparation method of 4′-*C*-substituted purine nucleosides from the corresponding nucleosides. This approach enabled us to synthesize 4′-*C*-cyano purine nucleoside derivatives, which were difficult to synthesize by condensation of sugars with nucleobases

Synthesis of 4′-C-cyano-2′-purine-nucleosides. The synthesis of 4′-*C*-cyano-2′-purine-nucleosides starting from 2′-deoxyadenosine and dDAP is shown (Figure 12). The key intermediates **[81a,b]** for the synthesis of 4′-*C*-ethynyl- and 4′-*C*-cyano-purine-2′-deoxynucleosides were prepared according to Matsuda's procedure, with some modifications (Nomura *et al.*, 1999). The hydroxymethyl group of the key intermediate **[81a]** was converted to a cyano group. A 4′-*C*-formyl derivative, which was obtained by Moffatt oxidation of the hydroxymethyl group in **[81a]**, was converted to a 4′-*C*-aldoxime derivative and then further dehydrated to give 4′-*C*-cyano derivative **[82a]**. The protecting groups of compound **[82a]** were removed to give 2′-deoxyadenosine derivative (4′-CNdA) **[83a]**. Additionally, 4′-*C*-cyano-2,6-diaminopurine 2′-deoxyriboside (4′-CNdDAP) **[83b]** was also synthesized by a similar procedure to that described for compound **[83a]**. The cyano derivatives **[83a,b]** were readily converted to 2′-deoxyinosine (4′-CNdI) **[84a]** and 2′-deoxyguanosine derivatives (4′-CNdG) **[84b]** by enzymatic deamination.

Synthesis of 4′-EdNs from 2′-deoxynucleosides. These synthetic methods using nucleosides as the starting material were also an effective route to the various 4′-*C*-ethynyl derivatives 4′-EdA **[86a]**, 4′-EdI **[87a]**, 4′-EdDAP **[86b]** and 4′-EdG **[87b]** (Figure 12). It will be easy for us to scale up the process for the preparation of 4′-*C*-ethynyl derivatives.

In summary, we developed a method for preparing purine 2′-deoxynucleoside derivatives bearing an ethynyl or a cyano group at the 4′ position from the corresponding 2′-deoxynucleosides as the starting materials. The total yields of 4′-*C*-substituted purine nucleosides were improved (compared to that of the condensation method of sugars with bases) by using this synthetic route. Furthermore, it became easy to make derivatives bearing an electron-withdrawing substituent like a cyano group.

Anti-HIV activity of 4′-CNdNs. The activity of 4′-CNdNs, together with that of 4′-EdNs, is shown in Table 2. Unfortunately, the anti-HIV activity of 4′-CNdNs did not meet our expectations. In the case of 4′-EdA **[86a]**, it was easily hydrolysed to give 4′-EdI **[87a]**, which was less active than the parent 4′-EdA **[86a]**. In contrast, 4′-CNdI **[84a]** was as potent as 4′-CNdA **[83a]** against HIV-1 despite the low activity of 4′-EdI **[87a]**.

Attempts to synthesize less toxic and/or stable analogues

Design and synthesis of L-4′-EdNs (L-4′-EdDAP [92], dG [93], and dC [98]). During our exploration of novel NRTIs, we selected 4′-ethynyl-2′-deoxy-purine-nucleoside (2,6-diaminopurine derivative **[86b]** and guanine derivative **[87b]**) for *in-vivo* assay because of their high biological activity *in vitro*. However, they showed high toxicity in mice (Ashida, Yamasa Corporation, personal communication). Additionally, 4′-*C*-cyano-2′-deoxy-purine-nucleoside (2,6-diaminopurine derivative **[83b]** and guanine derivative **[84b]**) were very toxic in the *in-vitro* assay (Ashida, Yamasa Corporation, personal communication). On the other hand, Chu *et al.* reported that the enantiomer of 3TC (D-enantiomer) was very toxic, but 3TC itself (L-enantiomer) was less toxic (Beach *et al.*, 1992). Therefore, we designed and synthesized L-4′-ethynyl derivatives such as **[92]** and **[93]** in an effort to reduce toxicity (Figure 13) (Kitano, Yamasa Corporation, private communication). Synthesis of the L-ribose unit bearing an ethynyl group at the 4-*C*-position and the glycosidation are outlined (Figure 13).

Table 2. Anti-HIV activity of 4'-C-cyano and 4'-C-ethynyl purine nucleosides

Compound	Anti-HIV activity*		
	EC_{50} (μM)	CC_{50} (μM)	Selectivity index
4'-ethynyl dA [86a]	0.0098	16	1633
4'-ethynyl dDAP [86b]	0.00034	0.9	2647
4'-ethynyl dI [87a]	0.13	137	1054
4'-ethynyl dG [87b]	0.0015	1.4	933
4'-cyano dA [83a]	0.051	12	235
4'-cyano dDAP [83b]	0.00079	>0.034	>43
4'-cyano dI [84a]	0.051	23	451
4'-cyano dG [84b]	0.000188	>0.034	>181
zidovudine (AZT)	0.0032	29.4	9188

*Anti-HIV activity was determined by MTT assay. MT-4 cells and $HIV\text{-}1_{LAI}$ were employed.

Figure 12. Synthesis of 4'-C-cyano and 4'-C-ethynyl purine 2'-deoxynucleosides by modification of natural nucleosides

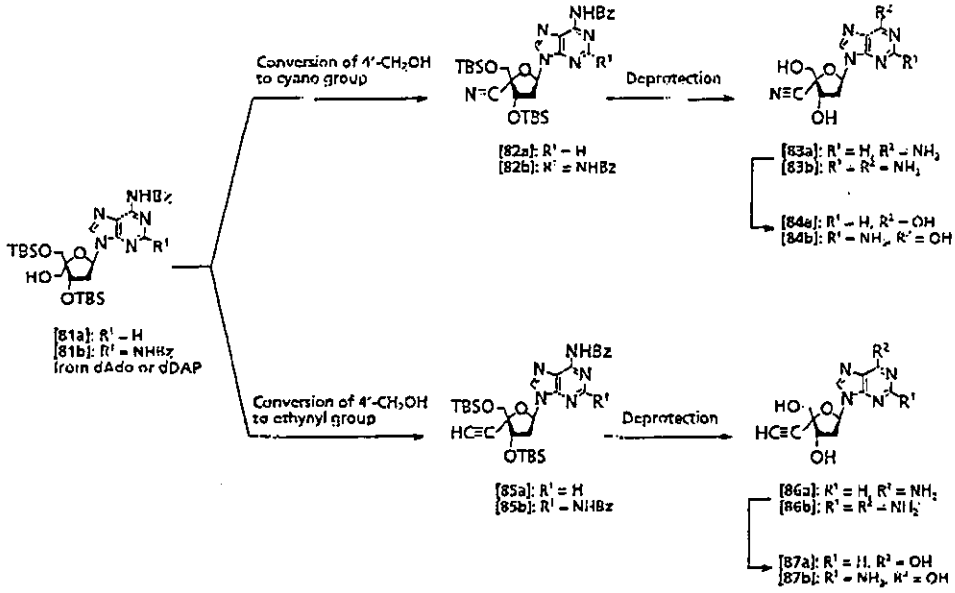

4-C-Hydroxymethyl-3,5-di-O-benzyl-1,2-O-isopropylidene-α-L-ribo-pentofuranose [89]. The key intermediate, was obtained from D-arabinose in nine steps. Silylation and isopropylidenation of D-arabinose gave 5-*O*-TBDPS-1,2-*O*-isopropylidene-α-D-*arabino*-pentofuranose **[88]** in two steps. The inversion of the 3-hydroxyl group in compound **[88]** gave D lyxo-pentofuranose derivative, which was derived to the key intermediate **[89]** by introduction of a hydroxymethyl group into the *C*-4 position by Moffatt's procedure and the following selective benzylation of the 5-hydroxyl group. L-Enantiomers of 4′-*C*-ethynyl dDAP **[92]** and dG **[93]** were obtained from the key intermediate **[89]** by a known procedure (Kohgo *et al.*, 1999; Ohrui *et al.*, 2000).

On the other hand, 4′-*C*-ethynyl-2′-deoxycytidine (4′-EdC) **[22]** had very potent anti-HIV activity, but this compound also showed cytotoxicity. Therefore, L-4′-*C*-ethynyl-2′-deoxycytidine (L-4′-EdC) **[98]** was also prepared from D-glucose by us (Figure 14) (Kohgo *et al.*, 2001) The synthetic scheme is summarized (Figure 14).

The L-enantiomers of 4′-*C*-ethynyl-2′-deoxynucleosides **[92, 93, 98]** were evaluated for anti-HIV activity toward MT-2 or MT-4 cells by an MTT assay. However, all these nucleosides were inactive against HTV-1 at concentrations up to 100 μM. It is worth noting none of the L-isomers of 4′-EdNs showed significant antiviral activity against HIV-1 *in vitro*.

Design and synthesis of 4′-C-substituted-6-chloropurine nucleosides (4′-S-6-CldNs) [101a,b] and 4′-C-substituted-6-mercapto-purine nucleosides (4′-S-6-SHdNs) [103a,b]. Additionally, we also chose 4′-EdA **[86a]** as another candidate because of its activity in the *in vitro* assay, but it was metabolized immediately *in vivo* to give the less active 4′-EdI **[87a]**. Thus, we attempted to resolve the above metabolic problem by a different approach. As mentioned above, while the anti-HIV activity of 4′-CNdNs did not meet our expectations, 4′-CNdI **[84a]** did prove active against HIV-1. Therefore, we focused on the modification at the 6-position of purine nucleosides in the case of 4′-ethynyl- and cyano-derivatives.

We previously confirmed that 6-chloro-purine-nucleosides were easily hydrolysed by adenosine deaminase (ADA) to give inosine derivatives. However, it was reported that 6-mercaptopurine-nucleosides were tolerant to this reaction (Murakami *et al.*, 1991). Furthermore, they also reported the modification method at the 6-position of purine dideoxynucleosides by chloro and mercapto groups to increase lipophilicity for these compounds (Murakami *et al.*, 1991). Therefore, we designed the modification at the 6-position of purine nucleosides utilizing their method. The preparation method for 4′-*C*-substituted 6-chloro-purine and 6-mercapto-purine derivatives is summarized in Figure 15.

We selected 4′-EdA derivative **[99a]** and 4′-CNdA derivative **[99b]** as key intermediates. The 6-amino group in 4′-EdA **[99a]** or 4′-CNdA derivatives **[99b]** were converted to a chloro group with Et_4NCl-tBuONO to give protected 6-chloro derivative **[100a,b]**. These derivatives **[100a,b]** were deprotected with ammoniumfluoride hydrogen fluoride (NH_4F-HF) in methanol or tetrabuthylammonium fluoride (TBAF) in THF to give the desired nucleosides **[101a,b]**.

Protected 6-chloro-purine derivatives **[100a,b]** were also used to prepare 6-mercapto-purine derivatives **[103a,b]**. Protected 4′-E- and 4′-CN-6-mercaptopurine analogues **[102a,b]** were obtained by the reaction of **[100a,b]** with sodium hydrosulphide in distilled water/ethanol or thiourea in refluxing ethanol, and the following deprotection of **[102a,b]** gave 4′-E- and 4′-CN-6-mercaptopurine derivatives **[103a,b]**.

Unfortunately, while 6-Cl purine derivative **[101a,b]** still showed weak activity, 6-mercapto derivatives **[103a,b]** exerted no anti-HIV-1 activity *in vitro*. The lack of antiretroviral activity of these nucleosides **[101a,b; 103a,b]** may be due to them not being converted to the desired analogues of 4′-*C*-substituted dG or dI. According to Murakami *et al.*, (1991) 2-amino-6-mercapto-ddNs are not substrates for ADA nor is it converted to ddG at all in the presence of an excess of isolated ADA.

Design and synthesis of α-L-4′-CNdNs (Kohgo, Yamasa Corporation, private communication). Inversion of the configuration at the 4′-*C* of the sugar leads to the α-L-series of nucleosides; therefore, we made alpha-L-4′-*C*-cyano-2′-deoxyadenosine. Unfortunately, α-L-4′-CNdNs did not show anti-HIV activity. Synthesis in our laboratory of α-L-4′-EdNs is in progress.

As can be seen from the results mentioned above, 4′-*C*-ethynyl- and 4′-cyano-nucleosides are promising candidates among various 4′-*C*-substituted nucleosides. Therefore, finally we describe the crucial factors (drug resistance, stability, mode of actions, toxicity and bulkiness) which will influence the development of the 4′-*C*-ethynyl-nucleosides and other 4′-SdNs.

Drug resistance

Activity of 4′-SdNs against drug-resistant infectious HIV-1 clones

The activity of selected 4′-SdNs against HIV-1 variants resistant to various NRTIs using MAGI assay is listed (Table 3). It is noteworthy that the three cytosine analogues, 4′-EdC **[22]**, 4′-EaraC **[79]** and 4′-MdC **[27]** suppressed the replication of HIV-1_{K65R}, HIV-1_{L74V}, HIV-$1_{M41L/T215Y}$ and multi-dideoxynucleoside-resistant HIV-$1_{A62V/V75I/F77L/F116Y/Q151M}$ (MDR) at EC_{50} values ranging

Figure 13. Synthesis of L-4′-C-ethynyl purine 2′-deoxynucleosides from D-arabinose

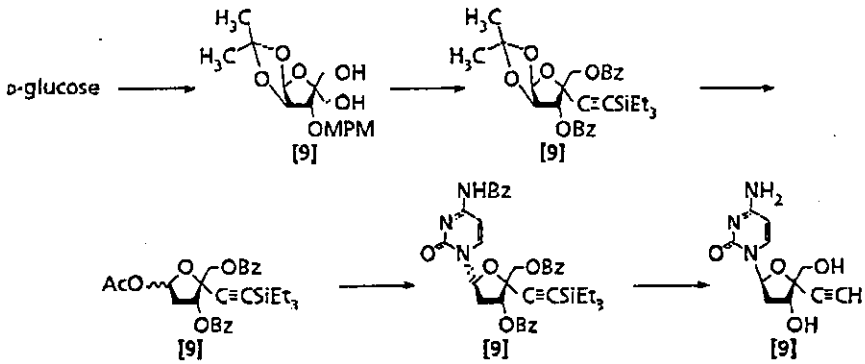

Figure 14. Synthesis of L-enantiomer of 4′-C-ethynyl-2′-deoxycytidine from D-glucose

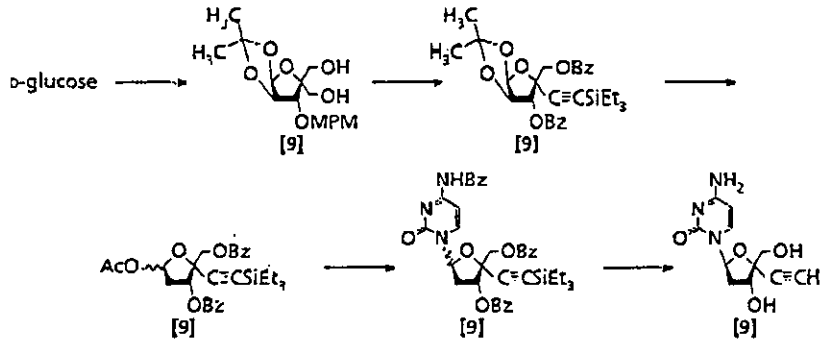

Table 3. Antiviral activity of 4'-C-substituted nucleosides against drug-resistant infectious clones

Compound	EC_{50} (μM)*									CC_{10} (μM)
	HXB2	K65R	L74V	M41L/T215Y	M184V	M184I	M41L/T69S-S-G/T215Y	MDR	Y181C	
Pyrimidine analogues										
4'-ET [28]	0.36	0.53	0.68	0.43	0.18	0.14	0.44	0.12	0.13	>200
4'-EdC [22]	0.0012	0.0008	0.0013	0.006	0.0024	0.0026	0.015	0.0012	0.0021	>200
4'-EaraC [79]	0.0071	0.015	0.026	0.026	0.71	0.48	0.17	0.0079	0.016	>200
4'-MdC [27]	0.0058	0.0071	0.0062	ND	0.2	0.74	ND	0.0033	ND	>200
4'-FMdC [73]	0.0046	0.065	0.0019	0.0035	2.0	ND	0.066	0.0039	ND	>200
Purine analogues										
4'-EdA [86a]	0.008	0.033	0.004	0.012	0.047	0.022	0.065	0.0062	0.011	>200
4'-EdDAP [86b]	0.0014	0.00035	0.0007	0.0017	0.0059	0.0027	0.0041	0.001	0.0008	>200
4'-EdI [87a]	0.81	0.25	0.61	1.3	16.6	1.5	2.2	0.51	ND	>200
4'-EdG [87b]	0.007	0.001	0.0012	0.019	0.008	0.0041	0.0068	0.0048	0.01	52
4'-CNdA [83a]	0.043	ND	ND	ND	2.28	ND	ND	0.083	ND	ND
4'-CNdI [84a]	0.242	ND	ND	ND	6.06	ND	ND	0.296	ND	ND
AZT	0.022	0.02	0.02	0.3	0.01	0.017	1.6	15.3	0.014	>100
ddC	0.2	3.0	1.5	ND	2.2	ND	1.3	5.5	ND	>100
3TC	0.71	ND	ND	ND	>100	>100	9.9	1.1	ND	>100
ddI	3.9	12.7	19.5	3.6	10.1	ND	12.2	25	ND	>100

*Anti-HIV activity was determined with the MAGI assay. ND, not determined.

Table 4. Antiviral activity of 4'-C-ethynyl nucleosides against clinical isolates

Strain	Amino acid substitution(s)		EC_{50} (μM)*			
	RT region	Protease region	4'-EdC [22]	4'-EdA [86a]	4'-EdDAP [86b]	AZT
ERS_{104pre}	None	None	0.0012	0.013	0.00083	0.0056
IVR_{203}	None	K20M, M36I, D60E	0.0023	0.0034	0.0001	0.0015
IVR_{207}	G190Q	V77I	0.0046	0.0022	<0.0001	0.0036
Pt1	T69G, K70R, L74V, A98G, K103N, V179D, M184V, T215F, K219F	L10I, L33I, M36I, M46I, L36P, A71V, G73S, V82A, L90M	0.00064 (0.5-fold)	0.00054 (0.4-fold)	0.0011 (1.3-fold)	0.029 (52-fold)
Pt6	M41L, D67N, M184V, L210W, T215Y	L10I, K20R, L24I, M36I, M46L, I54V, L63P, V82A, L89M	0.013 (11-fold)	0.040 (3-fold)	0.0001 (0.1-fold)	0.28 (50-fold)
Pt7	M41L, D67N, T69D, M184V, T215F	L10I, K45R, I54V, L63P, A71V, V82T, L90M	0.0016 (1.3-fold)	0.009 (0.7-fold)	0.0005 (0.6-fold)	1.9 (340-fold)
Pt9	M41L, M184V, T215Y	M46I, L63P, A71V, V77I, I84V, N88D, L90M	0.023 (19-fold)	0.029 (2.2-fold)	0.0031 (3.7-fold)	0.97 (170-fold)

*EC_{50}s were determined with PHA-PBMC. Numbers in parentheses represent fold changes of EC_{50}s against each HIV-1 isolate compared to those against the wild-type clinical HIV-1 strain, ERS_{104pre}.

from 0.001–0.015 μM. Among these nucleosides, only 4′-EdC [22] remained active against 3TC-resistant HIV-1_{M184I} and HIV-1_{M184V} but was less active against MDR-HIV-$1_{M41L/T69S-S-G/T215Y}$ than other variants, while 4′-EdC [22] remained potent against MDR-HIV-$1_{M41L/T69S-S-G/T215Y}$. The three purine analogues (4′-EdA) [86a], 4′-EdDAP [86b] and 4′-EdG [87b] that were potent against wild-type HIV-1 were also highly active against all the infectious clones. Additionally, they were also active against a non-nucleoside RTI-resistant (NNRTI) infectious HIV-1_{Y181C}.

Activity of 4′-SdNs against HIV-1 isolated from heavily drug-experienced patients with AIDS

The *in vitro* activity of the three most potent 4′-E-nucleosides (Table 4), 4′-EdC [22], 4′-EdA [86a] and 4′-EdDAP [86b] was tested against multi-drug resistant clinical HIV-1 variants isolated from heavily drug-experienced patients with AIDS. All three 4′-E-nucleosides suppressed replication of these highly drug-resistant clinical strains isolated from patients 1 and 7 as effectively as those of the wild-type clinical strain HIV-$1_{ERS104pre}$.

Properties and pharmacokinetics of 4′-EdNs and 4′-CNdNs

Stability of 4′-SdNs against enzymatic catabolism. It took 4 h to completely deaminate 4′-EdA [86a]. Under the same conditions, the enzyme, adenosine deaminase, deaminated ddA in 2 h. Pyrimidine phosphorylase hydrolysed 4′-*C*-methyl-2′-deoxy-5-ethyluridine by only 6% under conditions where the enzyme hydrolysed arabinofuranosyl-5-ethyluridine by 53% and 2′-deoxy-5-ethyl-uridine completely. All attempts for enzymatic exchange of the base of 4′-ET [28] with adenine were unsuccessful because the glycosyl linkage of 4′-ET [28] was too stable to be cleaved by the enzymes used. 4′-SdNs are fairly stable under physiological conditions, although the catabolism of 4′-SdNs following triphosphorylation as yet remains to be determined.

Stability of 4′-SdNs (mainly 4′-EdNs) under acidic conditions. When three 4′-EdNs (4′-EdC 22, 4′-EdA) [86a], and 4′-EdDAP [86b] and two ddNs (ddI and AZT) were exposed to 1M HCl for up to 20 min and then to 1M NaOH, their anti-HIV-1 activity was then tested. All 4′-EdNs were active although the acid-labile ddI completely lost its antiviral activity. The acid-stable property of these 4′-SdNs may contribute favourably to their oral bioavailability, if they are ultimately administered orally.

Mode of actions of 4′-SdNs. 4′-SdNs act as NRTIs and terminators of viral DNA biosynthesis in spite of the presence of the 3′α-OH group. Although a variety of side effects of NRTIs, some of which are often lethal, are well known and attributed to the inhibitory effect of ddN-TPs on mitchondrial polymerase γ activity, such effect has yet to be determined for 4′-SdNs. Such data regarding polymerase γ inhibition of 4′-SdNs-TPs are essential before 4′-SdNs may be considered as potential therapeutics for HIV-1 infection.

4′-E-nucleosides examined in our study retain the 3′-OH moiety like natural substrates, which may enable 4′-E-nucleosides to interact with the mutated 3′-OH binding site of various types of drug-resistant HIV.

Toxicity. It should be noted, however, since 4′-SdNs have the 3′-OH moiety, that the incorporation of 4′-SdNs to cellular and mitochondrial DNA may be more likely to happen, thus causing higher levels of unacceptable toxicity compared with ddNs. 4′-EdDAP [86b], 4′-EdG [87b], 4′-CNdDAP [83b] and 4′-CNdG [84b] were very toxic. Fortunately, 4′-EdA [86a], 4′-EdI [87a], 4′-CNdA [83a] and 4′-CNdI [84a] were less toxic.

Bulkiness. The results indicate that the structures of 4′-SdNs with a less sterically demanding substituent at the 4′-position are closer to the structures of dNs and have greater anti-HIV activity. However, the 4′-CN derivative did not meet our expectations. The expected properties come from the presence of 4′-substituents.

Conclusions

As can be seen from the research histories of various 4′-SdNs, novel NRTIs such as either 4′-EdNs (by us) and 4′-Ed4T [47] (by M Tanaka's group) appear to have sufficient anti-HIV-1 potency and favourable pharmacological properties. Therefore, they may be promising candidate therapeutics for HIV-1 infection and may be active against presently existing drug-resistant HIV-1 strains.

It should be noted that several issues, such as inhibition of mitochondrial DNA synthesis by 4′-SdNs-TPs (due to polymerase γ inhibition by 4′-SdNs-TPs) and pharmacokinetics, remain to be addressed before these analogues are considered for further development. However, we believe that NRTIs, especially 4′-EdNs, 4′-CNdNs and 4′-Ed4T [47], may be considered as potential therapeutics for HIV-1 infection. It is also noteworthy that 4′-Ed4T [47] is less toxic to CEM cell growth and less inhibitory to mitochondrial DNA synthesis than d4T. Further searches for NRTIs are in progress in our laboratory.

Acknowledgements

The authors are grateful to Dr K Kodama of Yamasa Corporation for his encouragement throughout this work. Thanks are also due to Dr T Waga, Dr S Sakata, Dr K

Figure 15. 4′-C-substituted 6-chloro and 6-mercapto purine nucleosides

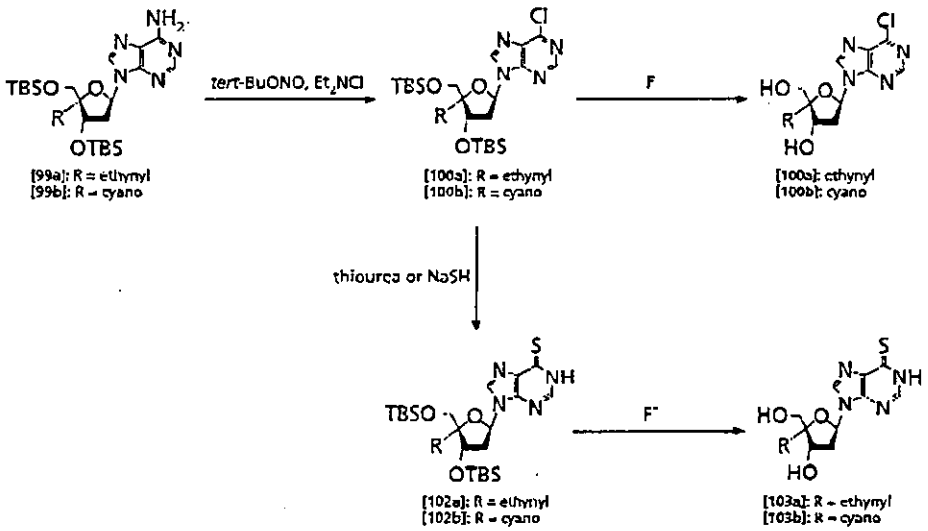

Yamada, Mr N Matsumoto for synthetic experiments, Dr S Shigeta, Dr M Saneyoshi, Dr T Yamaguchi, Dr M Matsuoka, Mr D Nameki, Dr T Abiru and Dr H Machida for biological studies.

References

Beach JW, Jeong LS, Alves AJ, Pohl D, Kim HO, Chang C-N, Doong S-L, Schinazi RF, Cheng Y-C & Chu CK (1992) Synthesis of enantiomerically pure (2′R, 5′S)-(-)-1-[2-(hydroxymethyl)oxathiolan-5-yl]cytosine as a potent antiviral agent against hepatitis B virus (HBV) and human immunodeficiency virus (HIV). *Journal of Organic Chemistry* 57:2217–2219.

Chen MS, Suttmann RT, Papp E, Cannon PD, McRoberts MJ, Bach C, Copeland WC & Wang TS (1993) Selective action of 4′ azidothymidine triphosphate on reverse transcriptase of human immunodeficiency virus type 1 and human DNA polymerases alpha and beta. *Biochemistry* 32:6002–6010.

Crich D & Hao X (1999) Asymmetric synthesis of C4′α-carboxylated 2′-deoxynucleosides. Preparation of oxetanone derivatives and influence of solvent on the stereochemistry of base introduction. *Journal of Organic Chemistry* 64:4016–4024.

Haraguchi K, Itoh Y, Takeda S, Honma Y, Tanaka H, Nitanda T, Baba M, Dutschman GE & Cheng Y-C (2004) Synthesis of anti-HIV activity of agent 4′-cyano-2′, 3′-didehydro-3′-deoxythymidine. *Nucleosides Nucleotides & Nucleic Acids* 23:647–654.

Haraguchi K, Takeda S, Tanaka H, Nitanda T, Baba M, Dutschman GE & Cheng Y-C (2003) Synthesis of a highly active new anti-HIV agent 2′,3′-didehydro-3′-deoxy-4′-ethynylthymidine. *Bioorganic & Medicinal Chemistry Letters* 13:3775–3777.

Haraguchi K, Tanaka H, Ito Y, Saito S & Miyasaka T (1992) Stereoselective synthesis of 4′-*C*-branched 2′,3′-didehydro-2′,3′-dideoxy nucleosides based on SnCl4-promoted allylic rearrangement. *Tetrahedron Letters* 33:2841–2844.

Hrebabecky H & Holy A (1993) Synthesis of 1-(3-azido-2, 3-dideoxy-4-*C*-hydroxymethyl-α-L-threo-pentofuranosyl)thymine, 1-(2,3-dideoxy-4-*C*-hydroxymethyl-α-L-glycero-pentofuranosyl)thymine and 1-(2,3-dideoxy-4-*C*-hydroxymethyl-α-L-glycero-pent-2-enofuranosyl)thymine. *Collection of Czechoslovak Chemical Communications* 58:409–420.

Imanishi T & Obika S (1999) Syntheses and properties of novel conformationally restrained nucleoside analogues. *Journal of Synthetic Organic Chemistry Japan* 57:969–980.

Jenkins ID, Verheyden, JPH & Moffatt JG (1976) 4′-Substituted nucleosides. 2. Synthesis of the nucleosides antibiotic nucleocidine. *Journal of the American Chemical Society* 98:3346–3357.

Johnson CR, Esker JL & Van Zandt MC (1994) Chemoenzymatic synthesis of 4-substituted riboses. S-(4′-methyladenosyl)-L-homocysteine. *Journal of Organic Chemistry* 59:5854–5855.

Jones GH, Taniguchi M, Tegg D & Moffatt JG (1979) 4′-Substituted nucleosides. 4. Synthesis of some 4′-hydroxymethyl nucleosides. *Journal of Organic Chemistry* 44:1309–1317.

Jung ME & Toyota A (2001) Preparation of 4′-substituted thymidines by substitution of the thymidine 5′-esters. *Journal of Organic Chemistry* 66:2624–2635.

Kato K, Suzuki H, Tanaka H & Miyasaka T (1998) Enantio- and diastereoselective synthesis of 4′-α-substituted carbocyclic nucleosides. *Tetrahedron: Asymmetry* 9:911–914.

Kitano K, Machida H, Miura S & Ohrui H (1999) Synthesis of novel 4′-*C*-methyl-pyrimidine nucleosides and their biological activities. *Bioorganic & Medicinal Chemistry Letters* 9:827–830.

Kitano K, Miura S, Ohrui H & Meguro H (1997) Synthesis of 4′-*C*-fluoromethylnucleosides as potential antineoplastic agents. *Tetrahedron* 53:13315–13322.

Kodama E, Kohgo S, Kitano K, Machida H, Gatanaga H, Shigeta S, Matsuoka M, Ohrui H & Mitsuya H (2001) 4′-Ethynyl nucleoside analogs: potent inhibitors of multidrug-resistant human immunodeficiency virus variants *in vitro*. *Antimicrobial Agents & Chemotherapy* 45:1539–1546.

Kohgo S, Horie H & Ohrui H (1999) Synthesis of 4′-*C*-ethynyl-β-D-*arabino*- and 4′-*C*-ethynyL-2′-deoxy-β-D-ribo-pentofuranosyl pyrimidines, and their biological evaluation. *Bioscience Biotechnology & Biochemistry* 63:1146–1149.

Kohgo S, Kodama E, Shigeta S, Saneyoshi M, Machida H & Ohrui H (1999) Synthesis of 4′-substituted nucleosides and their biological evaluation. *Nucleic Acids Symposium Series* 42:127–128.

Kohgo S, Mitsuya H & Ohrui H (2001) Synthesis of the L-enantiomer 4′-*C*-ethynyl-2′-deoxycytidine. *Bioscience Biotechnology & Biochemistry* 65:1879–1882.

Kozak J & Johnson CR (1998) Synthesis of 4′-trifluoromethyl nucleoside analogs. *Nucleosides & Nucleotides* 17:2221–2239

Maag H, Rydzewski RM, McRoberts MJ, Crawford-Ruth D, Verheyden JPH & Prisbe EJ (1992) Synthesis and anti-HIV activity of 4′-azido- and 4′-methoxynucleosides. *Journal of Medicinal Chemistry* 35:1440–1451

Marx A, Erdmann P, Senn M, Körner S, Jungo T, Perrena M, Imwinkelried P, Dussy A, Kulicke KJ, Macko L, Zehnder M & Giese B (1996) Synthesis of 4′-*C*-acylated thymidines. *Helvetica Chimica Acta* 79:1980–1994.

Murakami K, Shirasaka T, Yoshioka H, Kojima E, Aoki S, Ford Jr. H, Driscoll JS, Kelley JA & Mitsuya H (1991) *Escherichia coli* mediated biosynthesis and *in vitro* anti-HIV activity of lipophilic 6-halo-2′,3′-dideoxypurine nucleosides. *Journal of Medicinal Chemistry* 34:1606–1612.

Nomura M, Shuto S, Tanaka M, Sasaki T, Mori S, Shigeta S & Matsuda A (1999) Nucleosides & Nucleotides 185 Synthesis and biological activities of 4′α-*C*-branched-chain sugar pyrimidine nucleosides. *Journal of Medicinal Chemistry* 42:2901–2908.

O-Yang C, Kurz W, Eugui EM, McRoberts MJ, Verheyden JPH, Kurz LJ & Walker KAM (1992) 4′-Substituted nucleosides as inhibitors of HIV: an unusual oxetane derivative. *Tetrahedron Letters* 33:41–44.

O-Yang C, Wu HY, Fraser Smith EB & Walker KAM (1992) Synthesis of 4′-cyanothymidine and analogs as potent inhibitors of HIV. *Tetrahedron Letters* 33:37–40.

Ohrui H, Kohgo S, Kitano K, Sakata S, Kodama E, Yoshimura K, Matsuoka M, Shigeta S & Mitsuya H (2000) Syntheses of 4′-*C*-ethynyl-β-D-*arabino*- and 4′-*C*-ethynyl-2′-deoxy-β-D-ribo-pentofuranosylpyrimidines and -purines and evaluation of their anti-HIV activity. *Journal of Medicinal Chemistry* 43:4516–4525.

Ohrui H & Mitsuya H (2001) 4′-*C*-Substituted-2′-deoxynucleosides: a family of retroviral agents which are potent against drug resistant HIV variants. *Current Drug Targets–Infectious Disorders* 1:1–10.

Ohrui H, Nishizaki T, Waga T & Meguro H (1991) Synthetic study on 4′-*C*-methyluucleosides: Part I, synthesis of 4-*C*-methyl-D-ribofuranose derivative. *Nucleic Acids Symposium Series* 25:1–2.

Owen GR, Verheyden, JPH & Moffatt JG (1976) 4′-Substituted nucleosides. 3. Synthesis of some 4′-fluorouridine derivatives. *Journal of Organic Chemistry* 41:1310–1317.

Prisbe EJ, Maag H, Verheyden JPH & Rydzewski RM (1993) Structure–activity relationships among HIV inhibitory 4′-substituted nucleosides. *Nucleosides & Nucleotides as Antitumor & Antiviral Agents*. Edited by CK Chu & DC Baker. New York: Plenum Press, pp. 101–113.

Secrist III JA & Winter Jr WJ (1978) Carbon-carbon bond formation at C_4' of a nucleoside. Synthesis and utilization of a uridine 4′,5′-enamine. *Journal of the American Chemical Society* 100:2554–2555.

Singh SK, Kumar R & Wengel J (1998) Synthesis of novel bicyclo[2.2.1]ribonucleosides: 2′-amino- and 2′ thio-LNA monomeric nucleosides. *Journal of Organic Chemistry* 63:6078–6079.

Sugimoto I, Shuto S, Mori S, Shigeta S & Matsuda A (1999) Nucleosides & Nucleotides 183. Synthesis of 4′α-branched thymidines as a new type of antiviral agent. *Bioorganic & Medicinal Chemistry Letters* 9:385–388.

Summerer D & Marx A (2001) DNA polymerase selectivity: sugar interactions monitored with high-fidelity nucleotides. *Angewandte Chemie International Edition* 40:3693–3695.

Thrane H, Fensholdt J, Renger M & Wengel J (1995) Novel linear and branched oligodeoxynucleotide analogues containing 4′-*C*-(hydroxymethyl)thymidine. *Tetrahedron* 51:10389–10402.

Verheyden, JPH & Moffatt JG. (1975) 4′-Substituted nucleosides. 1. Synthesis of 4′-methoxyuridine and related compounds. *Journal of the American Chemical Society* 97:4386–4395.

Waga T, Nishizaki T, Miyakawa I, Ohrui H & Meguro H (1993) Synthesis of 4′-*C*-methylnucleosides. *Bioscience Biotechnology Biochemistry* 57:1433–1438.

Waga T, Ohrui H & Meguro H (1996) Synthesis and biological evaluation of 4′-*C*-methylnucleosides. *Nucleosides & Nucleotides* 15:287–304.

Wang G, Middleton PJ, Lin C & Pietrzkowski Z (1999) Biophysical and biochemical properties of oligodeoxynucleotides containing 4′-*C*- and 5′-*C*-substituted thymidines. *Bioorganic & Medicinal Chemistry Letters* 9:885–890.

Wang G & Seifert WE (1996) Synthesis and evaluation of oligodeoxynucleotides containing 4′-*C*-substituted thymidines. *Tetrahedron Letters* 37:6515–6518.

Yamaguchi T, Tomikawa A, Hirai T, Kawaguchi T, Ohrui H & Saneyoshi M (1997) *Nucleosides & Nucleotides* 16:1347–1350.

Youssefyeh R, Tegg D, Verheyden, JPH, Jones GH & Moffatt JG (1977) Synthetic routes to 4′-hydroxymethylnucleosides. *Tetrahedron Letters* 18:435–438.

Youssefyeh RD, Verheyden, JPH & Moffatt JG (1979) 4′-Substituted nucleosides. 4. Synthesis of some 4′-hydroxymethyl nucleosides. *Journal of Organic Chemistry* 44:1301–1308.

Received 5 January 2004; accepted 31 March 2004

Corrections

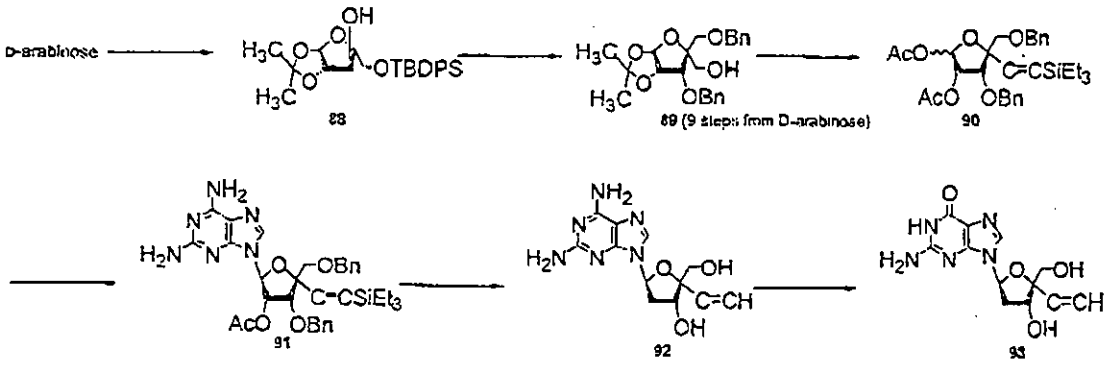

Figure 13. Synthesis of L-4'-C-ethynyl purine 2'-deoxynucleosides from D-arabinose

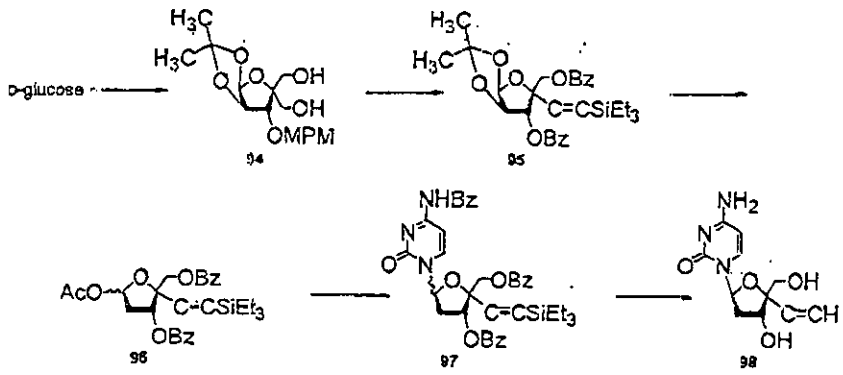

Figure 14. Synthesis of L-enantiomer of 4'-C-ethynyl-2'-deoxycytidine from D-glucose

[CANCER RESEARCH 64, 6002–6009, September 1, 2004]

Identification of Aberrantly Methylated Genes in Association with Adult T-Cell Leukemia

Jun-ichirou Yasunaga,[1] Yuko Taniguchi,[1] Kisato Nosaka,[1] Mika Yoshida,[1] Yorifumi Satou,[1] Tatsunori Sakai,[2] Hiroaki Mitsuya,[2] and Masao Matsuoka[1]

[1]Laboratory of Virus Immunology, Institute for Virus Research, Kyoto University, Kyoto, Japan; and [2]Department of Internal Medicine II, Kumamoto University School of Medicine, Kumamoto, Japan

ABSTRACT

In this study, we identified 53 aberrantly hypermethylated DNA sequences in adult T-cell leukemia (ATL) cells using methylated CpG island amplification/representational difference analysis method. We also observed a proportionate increase in the methylation density of these regions with disease progression. Seven genes, which were expressed in normal T cells, but suppressed in ATL cells, were identified near the hypermethylated regions. Among these silenced genes, *Kruppel-like factor 4* (*KLF4*) gene is a cell cycle regulator and *early growth response 3* (*EGR3*) gene is a critical transcriptional factor for induction of Fas ligand (FasL) expression. Treatment with 5-aza-2′-deoxycytidine resulted in the recovery of their transcription, indicating that their silencing might be associated with DNA hypermethylation. To study their functions in ATL cells, we transfected recombinant adenovirus vectors expressing *KLF4* and *EGR3* genes. Expression of *KLF4* induced apoptosis of ATL cells whereas enforced expression of *EGR3* induced the expression of *FasL* gene, resulting in apoptosis. Thus, suppressed expression of *EGR3* enabled ATL cells to escape from activation-induced cell death mediated by FasL. Our results showed that the methylated CpG island amplification/representational difference analysis method allowed the isolation of hypermethylated DNA regions specific to leukemic cells and thus shed light on the roles of DNA methylation in leukemogenesis.

INTRODUCTION

Human T-cell leukemia virus type I (HTLV-I) is the causative retrovirus of a neoplastic disease, adult T-cell leukemia (ATL) and an inflammatory disease, HTLV-I-associated myelopathy/tropical spastic paraparesis (1–4). After infection with HTLV-I, a small proportion of carriers (about 2–5%) develop ATL after a long latent period (5). In this virus-induced leukemia, viral proteins encoded by HTLV-I play an important role in the proliferation of infected cells and leukemogenesis. Among them, Tax is considered to play a central role in leukemogenesis because of its pleiotropic actions (6, 7), such as transcriptional activation of cellular genes (8–10), *trans*-repression of cellular genes transcription (11, 12), and functional inactivation of p53 and MAD1 (12, 13). These pleiotropic functions render HTLV-I-infected cells able to proliferate, and confer resistance to apoptotic signals, resulting in clonal expansion.

In the late stage of leukemogenesis, *tax* is frequently inactivated through several mechanisms (14) such as loss of 5′-long terminal repeat (LTR) (15), genetic alterations of *tax* gene (16), and DNA hypermethylation in 5′-LTR (17), indicating that Tax is not always necessary for leukemogenesis. Because Tax is the major target molecule of CTLs *in vivo* (18), the expression of Tax confers a growth advantage to infected cells, but on the other hand, it renders infected cells susceptible to CTLs. Fully transformed ATL cells are considered to acquire the ability to proliferate *in vivo* in the absence of Tax expression. Such a transformation process is thought to include alterations of host genome: genetic and epigenetic changes. Although the genetic changes, such as mutation of *p53* (19) and deletion of *p16* (20, 21), in ATL cells were reported, they are not frequent and are observed predominantly in the late stage of the disease.

In addition to genetic alterations, DNA hypermethylation of promoter region CpG islands has been analyzed in the context of oncogenesis because this process silences gene transcription of tumor-suppressor genes. This epigenetic alteration is observed commonly in various cancer cells. Although methylation "profiling" studies have shown that some genes are frequently methylated in various tumor cells, other genes are methylated in a tumor-type-specific manner (22, 23). To date, several methods have been developed to isolate differentially methylated DNA regions in cancers (24–29). Recently, with methylated CpG island amplification/representational difference analysis (MCA/RDA) method, we isolated hypomethylated DNA regions and demonstrated that *MEL1S* gene was hypomethylated and aberrantly transcribed in ATL cells (30).

The present study was designed to isolate hypermethylated DNA regions in ATL cells compared with cells in the carrier state using the MCA/RDA method and to identify those genes that have an expression associated with DNA hypermethylation. On the basis of our results, we discuss the association between aberrant DNA methylation and leukemogenesis of ATL.

MATERIALS AND METHODS

Cells. Peripheral blood mononuclear cells (PBMCs) were isolated from 10 patients with ATL (five acute type cases and five chronic type cases), five asymptomatic carriers, and five uninfected individuals using Ficoll-Paque density centrifugation method. We also used the cell lines ED, ATL-43T, ATL-48T, ATL-55T, MT-1, and TL-Om1, which were derived from leukemic clones, and MT-2, which is derived from nonleukemic cells. To study the effect of demethylation, ATL-43T was cultured in media supplemented with 10 μmol/l 5-aza-2′-deoxycytidine (5-aza-dC; Sigma, St. Louis, MO) for 3 days, 10 μmol/l 5-aza-dC and 1 μmol/l trichostatin A (TSA; Sigma) for the last 24 hours, or 1 μmol/l TSA for 24 hours alone. The human embryonic kidney cell line, HEK 293, was used for the packaging of recombinant adenovirus vectors.

Viral FLICE-inhibitory protein (FLIP) derived from the equine herpes virus type 2, E8 (31), and the long form of murine cellular FLIP (mCasper$_L$; Ref. 32) expression vectors were transfected into ATL-43T cells by electroporation with a Gene Pulser II (Bio-Rad, Hercules, CA). Stable transfectants were selected and maintained in culture medium containing G418 (500 μg/ml; Nacalai tesque, Kyoto, Japan). The transfected cell lines by each of the vectors were designated as ATL-43T-E8 and ATL-43T-mCas, respectively.

Methylated CpG Island Amplification/Representational Difference Analysis. To identify aberrantly hypermethylated DNA regions in ATL cells, we used the MCA/RDA method, as reported previously (28). Five micrograms of genomic DNA were digested with 100 units of *SmaI* (New England Biolabs, Beverly, MA) twice and then digested once with 20 units of *XmaI* (New England Biolabs). RMCA adaptor was prepared by annealing of the oligonucleotides RMCA24 (5′-CCACCGCCATCCGAGCCTTTCTGC-3′) and

Received 4/26/04; revised 6/15/04; accepted 6/25/04.

Grant support: Grant-in-Aid for Scientific Research from the Ministry of Education, Science, Sports, and Culture of Japan.

The costs of publication of this article were defrayed in part by the payment of page charges. This article must therefore be hereby marked *advertisement* in accordance with 18 U.S.C. Section 1734 solely to indicate this fact.

Note: Supplementary data for this article can be found at Cancer Research Online (http://cancerres.aacrjournals.org).

Requests for reprints: Jun-ichirou Yasunaga, Laboratory of Virus Immunology, Institute of Virus Research, Kyoto University, Kyoto 606-8507, Japan. Phone: 81-75-751-4048; Fax: 81-75-751-4049; E-mail: jyasunag@virus.kyoto-u.ac.jp.

RMCA12 (5′-CCGGGCAGAAAG-3′), and ligated to the digested DNA fragments using T4 DNA ligase (New England Biolabs). To amplify the hypermethylated DNA fragments, which were ligated adaptors in both ends, PCR was performed using the RMCA24 oligonucleotides as primers. The amplicons were synthesized using samples from an ATL patient and a HTLV-I carrier. For detection of ATL cell-specific hypermethylated DNA sequences, MCA products from a carrier were used as a driver of RDA, and those products from an acute ATL patient as a tester. We used GeneFisher Basic Reagent Set (TaKaRa, Shiga, Japan) for RDA. In RDA step, 500 and 100 ng of ligation mixture were used for the first and second selective PCR, respectively. Oligonucleotides used for RDA were JMCA24 (5′-GTGAGGGTCGGATCTGGATGGCTC-3′), JMCA12 (5′CCGGGAGCCAGC-3′), NMCA24 (5′-GTTAGCGGACACAGGGCGGGTCAC-3′), and NMCA12 (5′-CCGGGTGACCCG-3′). Subcloning of the MCA/RDA products was carried out using pCR-XL-TOPO (Invitrogen, Carlsbad, CA) or pGEM-T Easy (Promega, Madison, WI) as vectors, and then the sequences of each fragment were determined by PCR using M13 primers. Sequence homologies and localization in chromosomes were identified using the BLAST program of the National Center for Biotechnology Information.[3]

MCA-Southern Hybridization. To confirm that the isolated DNA regions are specifically hypermethylated in ATL cells, Southern blot method was used. MCA products from an ATL patient and a HTLV-I carrier (500-ng each) were separated by electrophoresis in 1.5% agarose gels and then transferred to Hybond-N + (Amersham Biosciences, Piscataway, NJ). All of the isolated DNA fragments were labeled with ^{32}P, and hybridized to these filters.

Combined Bisulfite Restriction Analysis and Bisulfite Sequencing Analysis. For nine DNA regions identified by MCA/RDA, the methylation status of the DNA regions was determined by Combined Bisulfite Restriction Analysis or bisulfite sequencing as described previously (33). First, genomic DNAs were treated with sodium bisulfite (34) and then amplified by nested PCR using the specific primers listed in Supplementary Table 1. The PCR products of these regions were digested with *Taq*I (New England Biolabs) or *Acc*II (TaKaRa), subjected to electrophoresis in 3% agarose gels, and visualized by ethidium bromide staining. The percentage of DNA methylation was calculated by the intensities of methylation and unmethylation signal determined by ATTO densitometry software (ATTO, Tokyo, Japan).

For detailed analysis of DNA methylation in *Kruppel-like factor 4* (*KLF4*) and *early growth response 3* (*EGR3*) genes, we performed bisulfite sequencing. The PCR products of the isolated regions and promoter regions of these genes were subcloned into pGEM-T Easy, thereafter, the sequences of each of 10 clones were determined. Because the promoter sequence of *KLF4* has not been determined, we predicted its sequence using the program[4] supported by the BioInformatics & Molecular Analysis Section, Computational Bioscience and Engineering Lab, Center for Information Technology, and NIH. Primers for bisulfite sequencing are also listed in Supplementary Table 1.

Semi-quantitative Reverse Transcriptase-PCR. Total RNA was extracted from the PBMCs and cell lines using Trizol reagent (Invitrogen) and then treated DNaseI (Invitrogen). cDNAs were synthesized from 0.5 μg of total RNA with the Superscript First-Strand Synthesis System for reverse transcription (RT)-PCR (Invitrogen) and used for semi-quantitative RT-PCR as template. The primers used for RT-PCR and their annealing temperatures are summarized in Supplementary Table 2. The number of PCR cycles was appropriately determined for each quantification (Supplementary Table 2). We used 1.25 units of ExTaq polymerase (TaKaRa) for each reaction. All experiments were performed including samples of whole brain (Clontech, Palo Alto, CA) and skeletal muscle (Stratagene, La Jolla, CA) as positive control of PCR reaction.

Construction of Adenovirus Vectors. The recombinant adenovirus vectors containing *KLF4* and *EGR3* gene (KLF4-AD and EGR3-AD, respectively) were generated using Adeno-X Expression System (Clontech) according to the manufacturer's protocol. These adenovirus vectors were concentrated and purified by Virakit for adenovirus 5 and recombinant derivatives (Virapur, San Diego, CA), and then the viral titers were determined using Adeno-X Rapid Titer Kit (Clontech). The *lacZ*-containing adenovirus vector (lacZ-AD) was also prepared as a negative control. All adenovirus vectors were used to infect an ATL cell line, ATL-43T, at 1,000 infectious units/cell.

Flow Cytometric Analysis. The flow cytometry (model EPICS XL flow cytometer, Beckman Coulter, Miami Lakes, FL) was used for analyses of apoptosis. Annexin V-FITC/PI double staining and terminal-deoxynucleotidyl transferase-mediated dUTP-FITC nick-end labeling (TUNEL) assay were performed for detection of apoptosis, using MEBCYTO apoptosis kit (MBL, Nagoya, Japan) and MEBSTEIN apoptosis kit direct (MBL), respectively.

RESULTS

Isolation of Hypermethylated DNA Regions in the Genome from ATL Cells. To identify hypermethylated regions in the genome of ATL cells, we carried out MCA/RDA, which was used previously to isolate a number of methylated CpG islands in colon cancer cell line (28). MCA products were generated from the genomic DNA of a carrier (driver) and an acute ATL patient (tester). After the second round of RDA, the PCR products were subcloned, and their sequences were determined. To confirm that identified DNA fragments were amplified in tester amplicon, we examined whether isolated DNA fragment specifically hybridized to the tester amplicon using Southern blot method (MCA-Southern). Specific hybridization to the tester amplicon implied that isolated DNA regions were hypermethylated in ATL cells compared with peripheral blood mononuclear cell (PBMC) from a carrier. Finally, we identified 53 differentially hypermethylated DNA fragments in ATL cells. The chromosomal locations of all of the fragments were analyzed by NCBI BLAST program. We tested whether these identified regions satisfied the criteria for CpG islands proposed by Takai and Jones (35). The results revealed that the majority of clones (48 of 53 clones) were located in CpG islands. Information of isolated sequences is described in Table 1.

Accumulation of Aberrant DNA Hypermethylation during Disease Progression. Chronic ATL is characterized as an indolent form, which later progresses to aggressive forms (*i.e.*, acute or lymphoma-type ATL). To confirm that DNA hypermethylation identified in this study is associated with disease progression, we analyzed the extent of DNA methylation of nine DNA regions at different stages by Combined Bisulfite Restriction Analysis. Fig. 1*A* shows the profiles of the methylation status in these DNA fragments. In cell lines, CpG sites in identified DNA fragments were highly methylated, which was consistent with the finding of DNA methylation in the established cell lines. This confirmed that the isolated DNA regions were hypermethylated in ATL cells and that MCA-Southern could identify the hypermethylated DNA regions. In the carrier state, most DNA fragments were unmethylated. On the other hand, they were frequently methylated in chronic ATL, and the level of methylation increased in acute ATL, indicating that DNA methylation in the isolated DNA regions tends to accumulate according to disease progression. This was also confirmed in the sequential samples from a HTLV-I carrier, who developed acute ATL (Fig. 1*B*).

Identification of Genes near the Hypermethylated DNA Regions. To analyze the influence of identified DNA hypermethylation upon gene transcription, the neighboring genes were searched using NCBI BLAST program as described in Materials and Methods. We found that 31 of 53 (58%) clones were located within the exon or intron of the gene, and 41 of 53 (77%) loci were located within 10 kb from the transcriptional start site of the nearest gene (Table 1). Because the aberrant methylation of some identified genes, such as *PAX5* (clone 10; ref. 36) and *CSPG2* (clone 27; ref. 28), have been reported in various types of cancer cells, it confirmed that MCA/RDA method in this study isolated the hypermethylated DNA regions. Then, we analyzed the transcription of genes in which the transcriptional start sites existed within 2 kb from the identified hypermethylated DNA regions (Fig. 2). On the basis of their expression profiles, we could divide the genes identified into two groups; group I con-

[3] http://www.ncbi.nlm.nih.gov/BLAST/.
[4] http://bimas.dcrt.nih.gov:80/molbio/proscan/.

Table 1 *Characterization of DNA fragments isolated by MCA/RDA*

Clone	Size (bp)	Accession no. (location)	Chromosomal location	Nearest gene	CpG Island	Distance from TSS (bp)
1	733	NT_007592.13 (19499884–19500616)	6p21.31	*No gene**	Yes	
2	511	NT_006713.13 (6324465–6324975)	5q13.3	*OTP*	Yes	2,600
3	377	NT_025741.13 (5075242–5075619)	6q16.3	*SIM1*	Yes	5,800
4	486	NT_079617.1 (40630–41115)	4p16.1	*HMX1*	Yes	200
5	577	NT_016354.16 (9912331–9912907)	4q21.3	*NKX6–1*	Yes	700
6	418	NT_009237.16 (13859103–13859520)	11p15.2	*CALCB*	Yes	50
7	673	NT_011109.15 (19265899–19266571)	19q13.33	*No gene*	Yes	
8	746	NT_022184.13 (23995750–23996496)	2p21	*LOC375201*	Yes	7,600
9	923	NT_026437.10 (32654509–32655429)	14q22.1	*PTGDR*	Yes	40
10	894	NT_008413.16 (37015465–37016356)	9p13	*PAX5*	Yes	8,100
11	533	NT_030059.11 (38044642–38045174)	10q26.1	*EMX2*	Yes	5,300
12	651	NT_010505.14 (1424933–1425583)	16q12.1	*CBLN1*	Yes	680
13	568	NT_007592.13 (1276022–1276589)	6p24	*TFAP2A*	Yes	2,500
14	725	NT_008583.16 (25707371–25708095)	10q22.3	*MGC2555*	Yes	4,500
15	591	NT_079592.1 (49215607–49216197)	7p12.1	*LOC378069*	Yes	190
16	424	NT_023666.16 (1934093–1934516)	8p21.2	*No gene*	Yes	
17	806	NT_009237.16 (30583999–30584804)	11p13	*No gene*	Yes	
18	696	NT_016354.16 (58568060–58568755)	4q28.3	*PCDH10*	Yes	2,500
19	620	NT_079596.1 (7038723–7039342)	7q22	*LAMB1*	Yes	720
20	937	NT_007592.13 (17472263–17473201)	6p21.1	*No gene*	Yes	
21	462	NT_008183.17 (7857852–7858312)	8q11.23	*KIAA1889*	Yes	290
22	487	NT_008470.16 (11911721–11912207)	9q31	*KLF4*	Yes	1,100
23	893	NT_025741.13 (12657384–12658276)	6q21	*NR2E1*	Yes	690
24	750	NT_079592.1 (23721242–23721991)	7p15.1	*NPY*	Yes	370
25	766	NT_077451.3 (1864762–1865527)	5qter	*ADAMTS2*	Yes	1,800
26	607	NT_004610.16 (1272547–1273153)	1p35	*PLA2G2F*	No	2,600
27	404	NT_006713.13 (12160670–12161073)	5q14.3	*CSPG2*	Yes	960
28	521	NT_023666.16 (922959–923479)	8p21.2	*EGR3*	Yes	1,700
29	895	NT_029419.10 (19759986–19760882)	12q13.2	*NXPH4*	No	6,100
30	430	NT_079593.1 (2760886–2761315)	7q11	*No gene*	No	
31	476	NT_011362.8 (4369966–4370441)	20q12	*MAFB*	Yes	350
32	878	NT_033903.6 (11275620–11276497)	11q13.1	*RIN1*	No	550
33	732	NT_009755.16 (3985255–3985983)	12q24.32	*No gene*	Yes	
34	795	NT_026437.10 (16902942–16903736)	14q13	*LOC253970*	Yes	340
35	530	NT_004671.15 (9240059–9240588)	1q31	*LHX9*	Yes	920
36	724	NT_005334.14 (10987626–10988353)	2p24.1	*No gene*	Yes	
37	943	NT_009237.16 (31223373–31224306)	11p13	*WIT-1*	Yes	40
38	587	NT_077921.1 (573714–574300)	1p36.13	*PAX7*	Yes	660
39	273	BX649589.3 (5548–5821)	9q34.3	*AGS3*	Yes	6,100
40	755	NT_022184.13 (8050474–8051228)	2p23.3	*No gene*	No	
41	958	NT_010783.14 (18185717–18186674)	17q22	*TBX4*	Yes	200
42	871	NT_005403.14 (27236075–27236942)	2q31.1	*HOXD3*	Yes	1,300
43	470	NT_030059.11 (21731229–21731698)	10q24	*LBX1*	Yes	5,500
44	406	NT_008818.15 (769699–770104)	10q26.2	*LOC338623*	Yes	230
45	565	NT_023935.16 (8798224–8798788)	9q21	*No gene*	Yes	
46	526	NT_010194.16 (47422212–47422737)	15q23	*ISL2*	Yes	2,700
47	445	NT_029289.10 (9369340–9369784)	5q32	*ADRB2*	Yes	230
48	414	NT_023133.11 (17468804–17469217)	5q34	*NKX2–5*	Yes	2,600
49	583	NT_022792.16 (6841497–6842079)	4q33	*No gene*	Yes	
50	1096	NT_026437.10 (18598721–18599816)	14q13	*SSTR1*	Yes	1,500
51	608	NT_077812.2 (1002922–1003529)	19p13.3	*FLJ46061*	Yes	8,600
52	310	NT_006713.13 (1986840–1987149)	5q13.3	*No gene*	Yes	
53	465	NT_011512.9 (8031349–8031813)	21q21.1	*NCAM2*	Yes	690

Abbreviation: TSS, transcription start site.
* "*No gene*" means TSS of the nearest gene is more than 10 kb away from the isolated region.

tained genes with an expression that was observed in activated T lymphocytes but suppressed in HTLV-I-transformed and ATL cell lines (Fig. 2*A*). On the other hand, the transcription of genes in group II was not detected in activated T cells and HTLV-I-associated cell lines whereas their expression was found in the brain and/or skeletal muscle (Fig. 2*B*). Group II genes were hypermethylated only in ATL cells but not in normal T lymphocytes. These results suggest that the suppressed expression of group I genes is implicated in leukemogenesis.

Relationship between Silencing of Neighboring Genes and DNA Methylation. We studied the detailed DNA methylation status in the promoter and isolated regions of *KLF4* and *EGR3* genes, which belong to group I, using the bisulfite sequencing method. The sequences of each of the 10 clones are summarized in Fig. 3. In both ATL-43T and an acute ATL, the CpGs in the isolated region of *KLF4* gene, which existed in exon 3, were heavily methylated (Fig. 3*A*) whereas there was little methylation in normal PBMCs. In the predicted *KLF4* promoter sequence, there was dense DNA methylation in ATL-43T and mild methylation in fresh ATL cells whereas the CpGs in normal PBMC were little methylated (Fig. 3*A*). DNA methylation in the promoter region of *KLF4* has been studied in primary cells with different stage of ATL to analyze the association with disease progression (Fig. 3*B*). DNA methylation increased according to disease progression from carrier to leukemia although there was little difference between chronic and acute ATL. In the case of the *EGR3* gene, the isolated region, which was in exon 2, was hypermethylated in the ATL cell line and fresh ATL cells but hypomethylated in normal PBMC (Fig. 3*C*). Although the promoter region of *EGR3* was hypermethylated in the ATL cell line, it was not methylated in fresh ATL cells and normal PBMCs.

Next, we analyzed whether the transcriptions of these silenced genes could be recovered by the demethylating agent, 5-aza-dC, and/or a histone deacetylase inhibitor, TSA in ATL cells. The combination of 5-aza-dC and TSA is known to induce a synergistic effect on DNA demethylation (37). As shown in Fig. 2*C*, the transcripts of *KLF4* gene were re-expressed by 5-aza-dC alone or by combination

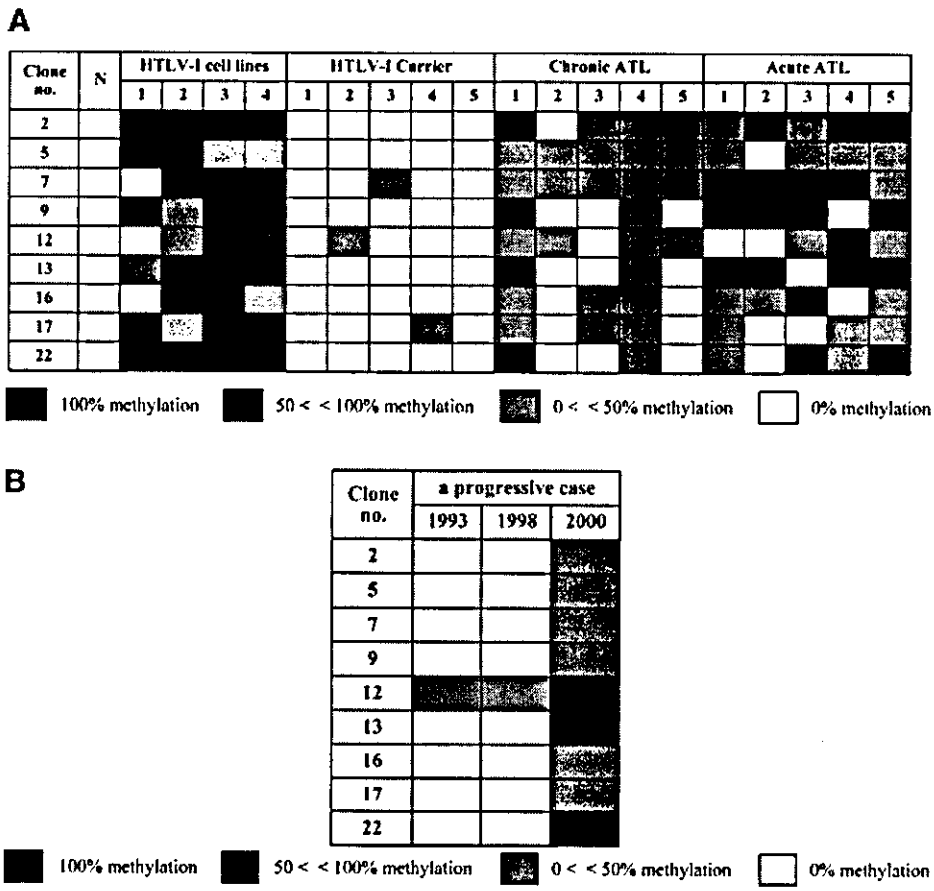

Fig. 1. Frequencies of CpG methylation of the isolated DNA regions in ATL cell lines and clinical samples. The frequencies of CpG methylation in 9 of 53 isolated regions were determined using the Combined Bisulfite Restriction Analysis method. *A*, methylation status in normal PBMCs (N), four ATL cell lines (*1*, MT-1; *2*, ATL-48T; *3*, ATL-43T; *4*, TL-Oml), and PBMCs from five asymptomatic HTLV-I carriers, five chronic ATL, and five acute ATL patients. Densities of methylation are represented by *tones of squares* as presented. *B*, serial changes of methylation status in these regions in a case with progression from carrier state to acute ATL.

treatment but not by TSA alone, suggesting that DNA methylation of *KLF4* gene is associated with its silencing in ATL cells. On the other hand, the transcript of *EGR3* gene was detected more clearly when ATL cells were treated with TSA alone or their combination than with 5-aza-dC alone, indicating that the *EGR3* gene was silenced by histone deacetylation rather than by DNA methylation. However, because demethylation by 5-aza-dC partially recovered *EGR3* gene transcription, we consider that DNA methylation is associated in part with suppressed expression of *EGR3* gene. In addition, the transcriptions of other group I genes, such as *CSPG2*, *MAFB*, and *ADRB2*, were also recovered by 5-aza-dC treatment. Because the transcription of *ADAMTS2* and *PTGDR* could not be recovered by either 5-aza-dC or TSA, the silencing of these genes might be because of other mechanism(s).

Enforced Expression of *KLF4* or *EGR3* Gene in ATL Cells. To investigate the function of *KLF4* and *EGR3* genes in ATL cells, adenovirus vectors expressing *KLF4* (KLF4-AD) or *EGR3* (EGR3-AD), were transfected into ATL-43T, in which the transcription of both genes were completely suppressed. Transfection of *KLF4*-expressing adenovirus vector induced the transcription (Fig. 4*A*) and resulted in accumulation of apoptotic cells as demonstrated by Annexin V-PI staining (Fig. 4*B*). The apoptosis was also confirmed by TUNEL assay (data not shown). The number of apoptotic cells reached maximum 48 hours later (30.1%, Fig. 4*C*). This percentage was similar to that of X-gal-stained cells (49.0%) when lacZ-AD was transfected into ATL-43T. Taken together, these results suggest that *KLF4* expression induced apoptosis in most transduced cells.

Because the *EGR3* gene is reported to be critical for *Fas ligand* (*FasL*) gene transcription (38), we studied whether enforced expression of *EGR3* could induce apoptosis of ATL cells. After transfection, both *EGR3* and *FasL* were transcribed 48 hours later (Fig. 5*A*), which coincided with increased apoptotic cells in ATL-43T infected EGR3-AD, in contrast to control (Fig. 5*B* and *C*). In addition, increased apoptotic cells were also confirmed by TUNEL assay (data not shown). Thus, enforced expression of EGR3 was considered to result in Fas-FasL-mediated apoptosis. To clarify whether this apoptosis is actually mediated by Fas signaling, we transfected vectors expressing $mCasper_L$ or E8. $mCasper_L$ is a mouse c-FLIP that inhibits the activation of procaspase 8 at the death-inducing signaling complex, whereas E8 is a viral FLIP derived from the equine herpes virus type 2. Transfection of EGR3-AD did not increase apoptosis of ATL-43T cells that expressed $mCasper_L$ and E8 (Fig. 5*A* and *C*), confirming that EGR3-induced apoptosis in ATL cell line is mediated by Fas-mediated signal.

DISCUSSION

In the present study, we identified hypermethylated DNA regions by MCA/RDA method. Consistent with the previous study (28), this method could identify hypermethylated CpG islands; 48 of 53 (91%) DNA clones identified in this study satisfied the criteria of CpG islands, and 41 of 53 (77%) DNA clones were located within 10 kb from the transcriptional start site of the nearest gene. Identified genes in the vicinity of isolated hypermethylated DNA regions could be divided into two groups; genes of group II are not expressed and not methylated in normal T lymphocytes, however, are hypermethylated in ATL cells. On the other hand, genes of group I are expressed but not methylated in normal T lymphocytes whereas their expression is suppressed in ATL cells in association with DNA methylation. It is possible that the mechanism of *de novo* methylation is dysregulated,

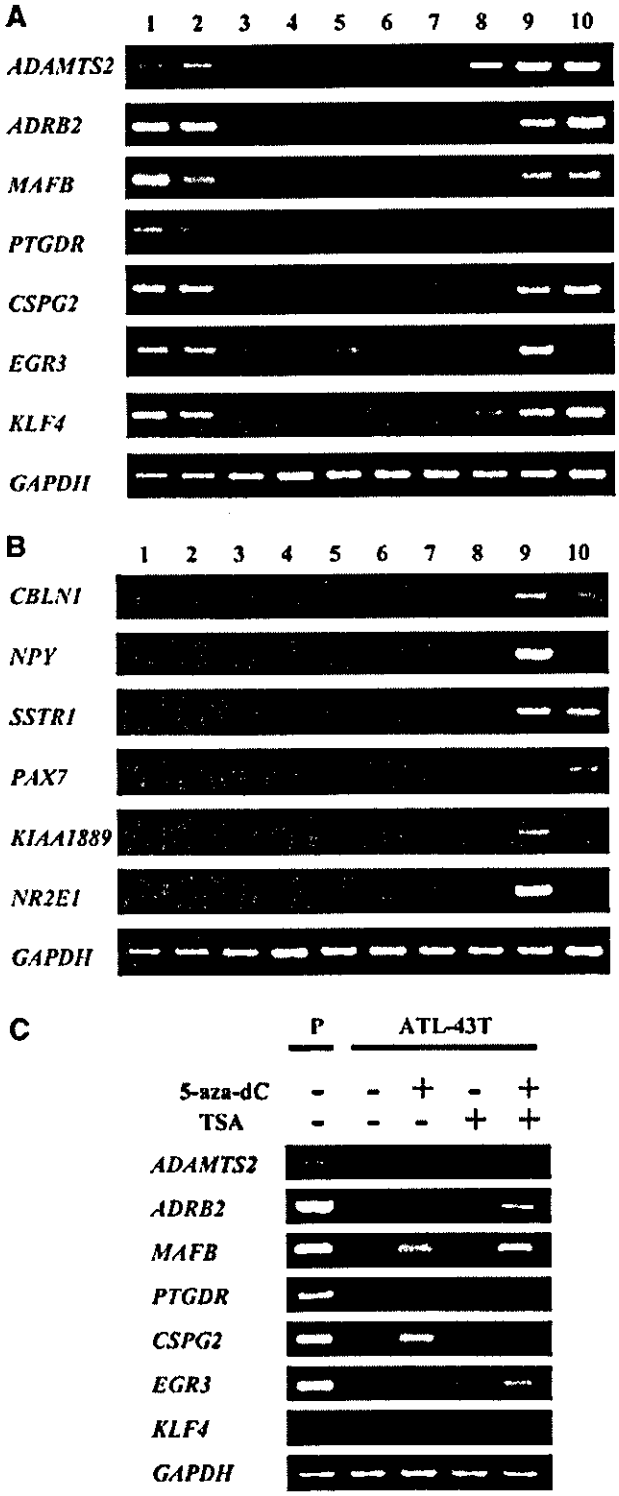

Fig. 2. Expression of genes in the vicinity of hypermethylated regions isolated by MCA/RDA. Expression of the genes near the isolated regions was studied by RT-PCR. Transcripts of the *glyceraldehyde-3-phosphate dehydrogenase* (*GAPDH*) gene were used as a control. *Lane 1*, normal resting PBMC; *Lane 2*, normal activated T cell; *Lane 3*, ED; *Lane 4*, ATL-43T; *Lane 5*, ATL-48T; *Lane 6*, ATL-55T; *Lane 7*, MT-1; *Lane 8*, MT-2; *Lane 9*, normal whole brain; *Lane 10*, normal skeletal muscle. *A*, group I, genes expressed in normal T cells but suppressed in HTLV-I-transformed and ATL cell lines. *B*, group II, genes not expressed in normal T cells and HTLV-I-associated cell lines. *C*, recovered expression of the group I genes after demethylation, ATL-43T was treated with 5-aza-dC only, TSA only, or both. Using cDNAs obtained from the treated and untreated cells, expressions of *KLF4* and *EGR3* were analyzed by RT-PCR. Phytohemagglutinin blast (P) was used as a positive control. RT-PCR of *GAPDH* was also performed to provide a control for initial RNA amounts.

resulting in aberrant methylation of genes despite their transcription as observed in group II genes. In this regard, Toyota *et al.* (28) isolated 33 hypermethylated DNA sequences in a colon cancer cell line using the MCA/RDA method and named these clones MINT1–33. Among DNA regions identified in this study, four clones were identical to MINT clones (Table 1, clone 2, clone 15, clone 30 and clone 48). These findings indicate that such DNA regions in the genome are prone to be methylated in cancer cells, which is consistent with an earlier report (22), although the factors that determine such susceptibility to methylation remain unresolved. In addition to such DNA methylation observed among different types of cancer cells, there are hypermethylated genes specifically observed in ATL cells. Analysis of DNA methylation of such genes in non-ATL T-cell lines showed that they were also methylated (data not shown), suggesting that DNA methylation of such genes is T-cell specific.

In addition to hypermethylation, we also reported hypomethylated genes in ATL cells, which included *MEL1S*, *CACNA1H*, and *Nogo receptor* genes as identified by the MCA/RDA method (30). Among them, the aberrant expression of *MEL1S* was frequently observed in ATL cells and has been shown to confer resistance against transforming growth factor-β. Thus, the MCA/RDA method indicates the involvement of both hyper- and hypomethylation in leukemogenesis of ATL although in a different manner.

In the case of *EGR3* gene, only the coding regions were methylated with little DNA methylation of the promoter region in fresh ATL cells although its expression was suppressed. TSA has more profound effect than 5-aza-dC, suggesting that histone modification, rather than DNA methylation, in the promoter region might silence the transcription of the *EGR3* gene. However, because DNA methylation in the coding region was associated with such silencing, detection of DNA methylation in non-promoter regions is also capable of identifying such silenced genes as observed in the *EGR3* gene.

EGR3 is a transcriptional factor containing zinc finger domain as well as KLF4. It has been reported that enforced expression of *EGR3* gene resulted in expression of *FasL* in HeLa cells (38), indicating that EGR3 is a critical transcriptional factor for *FasL* transcription. In agreement with these results, we also showed that expression of *EGR3* induced *FasL* transcription, resulting in apoptosis of ATL cells. Although ATL cells possess a phenotype of activated T cells and highly express Fas antigens on their surfaces, they do not produce FasL. On the other hand, normal T lymphocytes can express both Fas antigens and FasL after activation, and the number of activated T lymphocytes is regulated by Fas-FasL system-mediated apoptosis, which is designated as activation-induced cell death (39). Activation-induced cell death controls the number of activated T lymphocytes, consequently suppressing the immune response. Suppression of *EGR3* gene in ATL cells could account for lack of expression of FasL, which enables ATL cells to escape from activation-induced cell death. In the present study, we demonstrated that enforced expression of *EGR3* gene-induced FasL expression and apoptosis. Thus, because both KLF4 and EGR3 are accelerators of ATL cell apoptosis, *KLF4* and *EGR3* genes are considered new tumor-suppressor gene candidates in ATL.

KLF4 is a member of the Kruppel-like factor family, which is highly expressed in epithelial tissues such as the gut and skin, especially in the terminally differentiated cells (40, 41). Previous studies reported that KLF4 plays important roles in the regulation of G_1-S and G_2-M cell cycle checkpoint in colon cancer cells and that these functions are likely to be p53-dependent (42–44). According to these findings, KLF4 is thought to be associated with tumorigenicity of colon cancer cells. However, there is no report regarding the functional role of *KLF4* gene in lymphoid cells. Our study demonstrated that KLF4 expression induced apoptosis of ATL cells. Although the

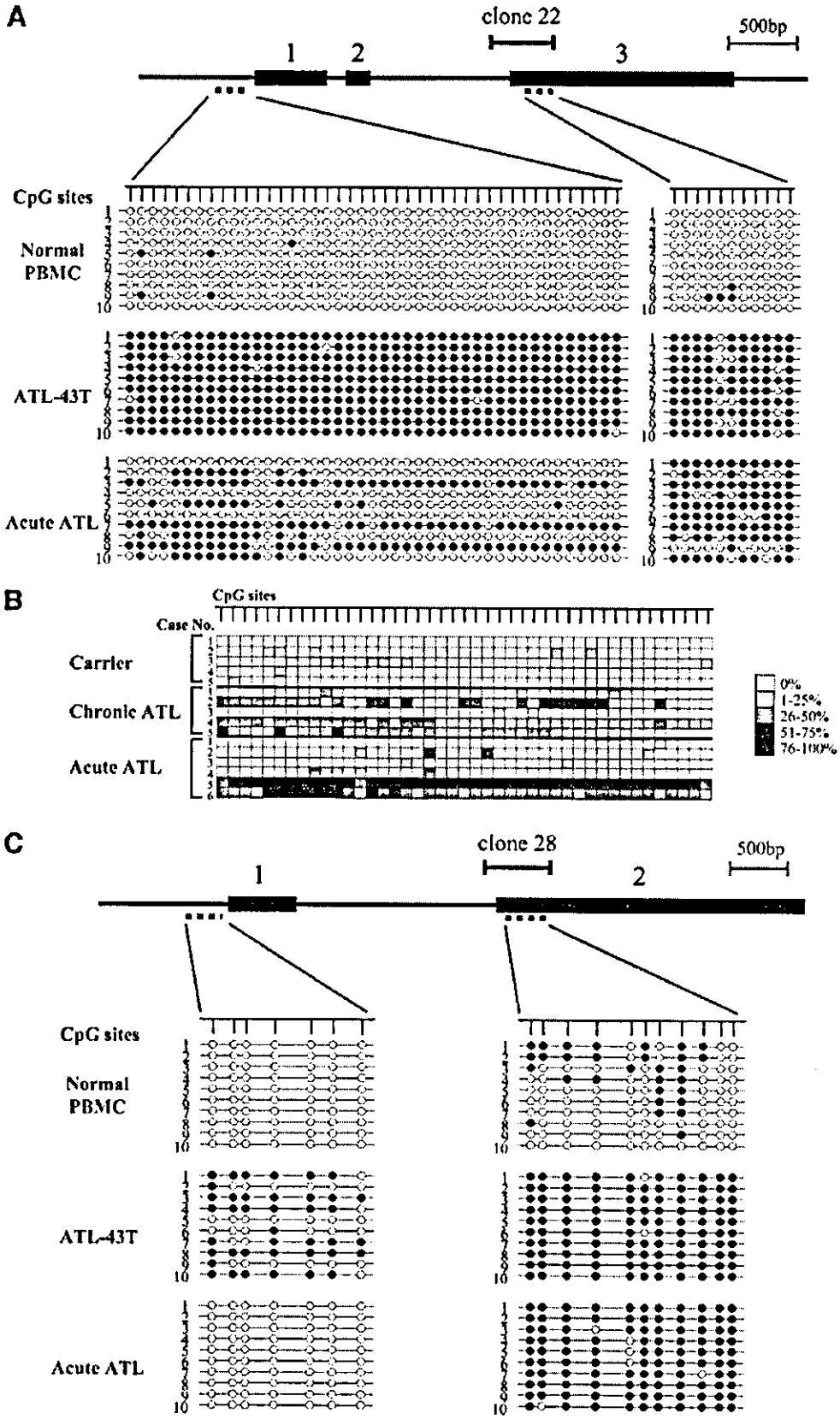

Fig. 3. Methylation status of *KLF4* and *EGR3* genes. Genomic DNAs of normal PBMC, an ATL cell line (ATL-43T), and primary cells of acute ATL were treated by sodium bisulfite and then amplified by primers specific for DNA regions in *KLF4* and *EGR3* genes identified by MCA/RDA and for their promoter regions. Then, PCR products were subcloned into plasmid DNA, and the sequences were determined in 10 clones of each (*A*, *KLF4*; *C*, *EGR3*). ○, unmethylated CpG sites; ●, methylated CpG sites. *B*, methylation status of *KLF4* promoter in primary cells with different stage of ATL; methylation level of each CpG site was calculated based on the results of bisulfite sequencing analysis and represented by *tones of squares*.

mechanism of apoptosis needs additional study, its silencing by DNA methylation facilitates the survival of ATL cells.

The present study showed that the densities of CpG methylation in identified DNA regions tend to increase with disease progression. Moreover, analysis of sequential samples from a patient who was followed from carrier state until the onset of acute ATL revealed that DNA methylation accumulated at the onset of ATL (Fig. 1*B*). These data indicate that serial analysis of the methylation status in identified hypermethylated regions might be a useful tool in the diagnosis and staging of ATL.

HTLV-I-infected clones have been shown to persist over seven years in the same HTLV-I carrier (45), suggesting that HTLV-I-infected cells survive for a long time through the action of viral proteins. On the other hand, it has been reported that aging is closely related to alterations of DNA methylation. Progressive loss of 5-methylcytosine content is observed in normal aging cells, primarily within DNA-repeated sequences. In contrast, some genes show progressive, age-related increases of DNA methylation, resulting in silencing their expressions (46). Taken together, the prolonged life span of HTLV-I-infected T cells might be a predisposing factor for aberrant DNA methylation. During the long latent period, it is possible that HTLV-I-infected cells that are adapted for survival are selected *in vivo*. In such evolution of infected cells, genetic and epigenetic changes are thought to play critical roles by suppressing the transcription of genes with tumor suppressor functions or activating the expression of genes, which exerts positive effects on survival of tumor cells.

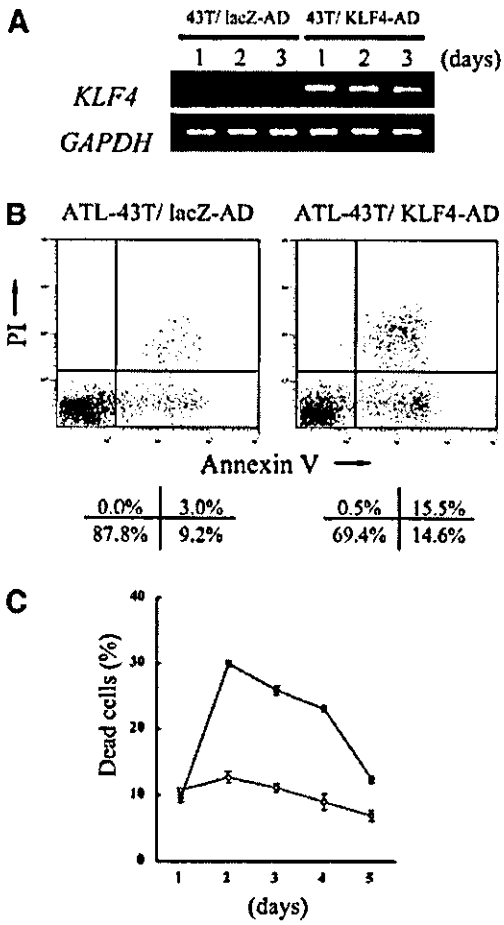

Fig. 4. Induction of apoptosis of ATL-43T by enforced expression of *KLF4*. *A*, expression of *KLF4* gene in ATL-43T transfected with lacZ-AD or KLF4-AD was studied by RT-PCR. *B*, detection of apoptotic cells in ATL-43T by double staining with Annexin V-FITC and PI at day 2 of lacZ-AD and KLF4-AD infection. The percentage of cells in each quadrant is shown at the *bottom of the panels*. *C*, serial changes in the percentages of dead cells detected by Annexin V-PI double staining. ○, ATL-43T infected with lacZ-AD; ●, ATL-43T infected with KLF4-AD. Data are mean ± SE.

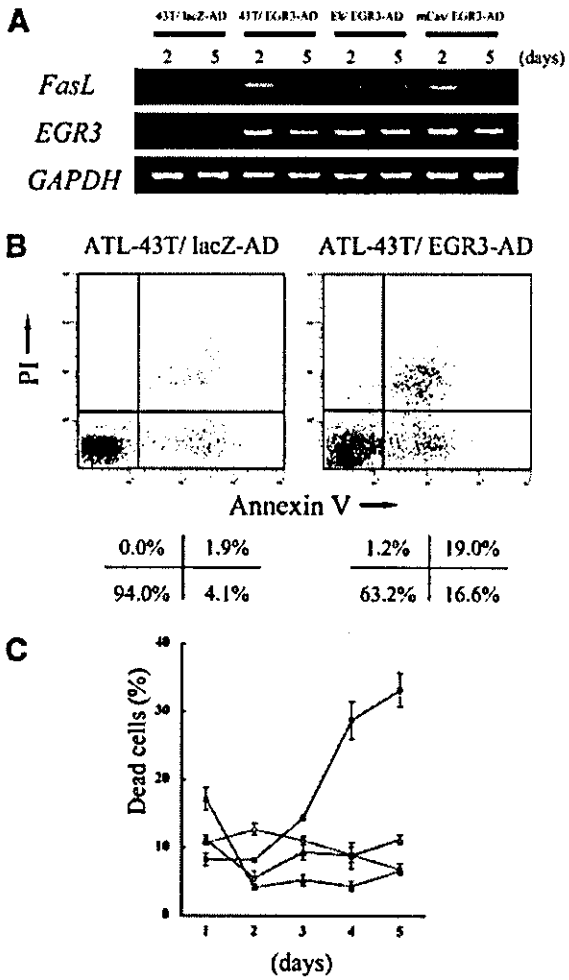

Fig. 5. Induction of *FasL* transcription and apoptosis of ATL-43T by enforced expression of *EGR3*. *A*, expressions of *EGR3* and *FasL* genes in transfected cell lines were studied by RT-PCR. *B*, detection of apoptotic cells in ATL-43T by double staining with Annexin V-FITC and PI at day 5 of lacZ-AD and EGR3-AD infection. The percentage of cells in each quadrant is shown at the *bottom of the panels*. *C*, serial changes in the percentages of dead cells detected by Annexin V-PI double staining. ○, ATL-43T infected with lacZ-AD; ●, ATL-43T infected with EGR3-AD; △, ATL-43T-mCas infected with EGR3-AD; and ▲, ATL-43T-E8 infected with EGR3-AD. Data are mean ± SE.

In conclusion, we have demonstrated in the present study that the MCA/RDA method could identify the differentially methylated DNA regions and genes according to disease progression of ATL. Such identification of aberrantly methylated genes allows for the diagnosis and staging of ATL and clarifies the molecular mechanism of leukemogenesis.

ACKNOWLEDGMENTS

We are grateful to Michiyuki Maeda for providing us valuable cell lines and to Yoshihiro Koya for valuable help. The authors also thank Dr. F. G. Issa (word-medex.com.au) for careful reading and editing of the manuscript.

REFERENCES

1. Takatsuki K, Uchiyama T, Sagawa K, Yodoi J. Adult T cell leukemia in Japan. In: Seno S, Takaku F, Irino S, editors. Topic in hematology: proceedings of the 16th international congress of Hematology, Kyoto, September 5–11, 1976. Amsterdam, Oxford: Excerpta Medica; 1977. p. 73–7.